A&A 576, L12 (2015)
DOI: 10.1051/0004-6361/201525865

Astronomy & Astrophysics

Letter to the Editor

Young [α/Fe]-enhanced stars discovered by CoRoT and APOGEE: What is their origin?⋆

C. Chiappini[1,2], F. Anders[1,2], T. S. Rodrigues[2,3,4], A. Miglio[5], J. Montalbán[4], B. Mosser[6], L. Girardi[2,3], M. Valentini[1], A. Noels[7], T. Morel[7], I. Minchev[1], M. Steinmetz[1], B. X. Santiago[2,8], M. Schultheis[9], M. Martig[10], L. N. da Costa[2,11], M. A. G. Maia[2,11], C. Allende Prieto[12,13], R. de Assis Peralta[6], S. Hekker[14,15], N. Themeßl[14,15], T. Kallinger[16], R. A. García[17], S. Mathur[18], F. Baudin[19], T. C. Beers[20], K. Cunha[11], P. Harding[21], J. Holtzman[22], S. Majewski[23], Sz. Mészáros[24,25], D. Nidever[26], K. Pan[22,27], R. P. Schiavon[28], M. D. Shetrone[29], D. P. Schneider[30,31], and K. Stassun[32]

(Affiliations can be found after the references)

Received 11 February 2015 / Accepted 18 March 2015

ABSTRACT

We report the discovery of a group of apparently young CoRoT red-giant stars exhibiting enhanced [α/Fe] abundance ratios (as determined from APOGEE spectra) with respect to solar values. Their existence is not explained by standard chemical evolution models of the Milky Way, and shows that the chemical-enrichment history of the Galactic disc is more complex. We find similar stars in previously published samples for which isochrone-ages could be reliably obtained, although in smaller relative numbers. This might explain why these stars have not previously received attention. The young [α/Fe]-rich stars are much more numerous in the CoRoT-APOGEE (CoRoGEE) inner-field sample than in any other high-resolution sample available at present because only CoRoGEE can explore the inner-disc regions and provide ages for its field stars. The kinematic properties of the young [α/Fe]-rich stars are not clearly thick-disc like, despite their rather large distances from the Galactic mid-plane. Our tentative interpretation of these and previous intriguing observations in the Milky Way is that these stars were formed close to the end of the Galactic bar, near corotation – a region where gas can be kept inert for longer times than in other regions that are more frequently shocked by the passage of spiral arms. Moreover, this is where the mass return from older inner-disc stellar generations is expected to be highest (according to an inside-out disc-formation scenario), which additionally dilutes the in-situ gas. Other possibilities to explain these observations (e.g., a recent gas-accretion event) are also discussed.

Key words. Galaxy: abundances – Galaxy: disk – Galaxy: formation – Galaxy: stellar content – stars: fundamental parameters – asteroseismology

1. Introduction

One of the pillars of Galactic Archaeology is the use of stellar [α/Fe] abundance ratios as an indirect age estimator: [α/Fe]-enhancement is an indication that a star has formed from gas enriched by core-collapse supernovae; longer-timescale polluters, such as supernovae of type Ia or asymptotic giant-branch stars, did not have sufficient time to enrich the interstellar medium (Pagel 2009; Matteucci 2001). High-resolution spectroscopy of the solar neighbourhood stars, for which Hipparcos parallaxes are available (e.g. Haywood et al. 2013), have indeed shown this paradigm to work well. One of the best examples is the very local (d < 25 pc) volume-complete sample of solar-like stars by Fuhrmann (2011, and references therein), for which it was possible to obtain robust isochrone ages for a small number of subgiants, which confirmed that stars exhibiting [α/Fe]-enhancements were all older than ~10 Gyr and identified them as thick-disc stars. Fuhrmann's data also show a clear chemical discontinuity in the [α/Fe] vs. [Fe/H] plane, which can be interpreted as the result of a star-formation gap between the thick and thin discs (Chiappini et al. 1997; Fuhrmann 2011).

However, as we demonstrate in this Letter, α-enhancement is no guarantee that a star is actually old. Only recently has it become possible to obtain more precise ages for field stars far beyond the solar circle, thanks to asteroseismology, with CoRoT (Baglin et al. 2006) and *Kepler* (Gilliland et al. 2010). Even more important, the CoRoT mission allows for age and distance determination of stars spanning a wide range of Galactocentric distances, as shown by Miglio et al. (2013a,b). The latter authors have shown that when asteroseismic scaling relations are combined with photometric information, mass and age can be obtained to a precision of about 10% and 30%, respectively, even for distant objects[1]. High-resolution spectroscopy of the seismic targets plays a key role, not only allowing for more precise ages and distances, but also providing full chemical and kinematical information.

We have initiated a collaboration between CoRoT and the Apache Point Observatory Galactic Evolution Experiment (APOGEE; Majewski et al., in prep.). APOGEE is a high-resolution (R ~ 22 000) infrared survey (λ = 1.51−1.69 μm) and part of the Sloan Digital Sky Survey III (SDSS-III; Eisenstein et al. 2011), which uses the Sloan 2.5 m telescope (Gunn et al. 2006). Here, we analyse data from the SDSS-III data release 12 (DR12; Alam et al. 2015), which contains 690 red-giant stars in the CoRoT fields LRa01 and LRc01 from an ancillary APOGEE campaign.

⋆ Appendix A is available in electronic form at http://www.aanda.org

[1] The quoted uncertainties in Miglio et al. (2013a) were computed assuming global seismic parameter uncertainties from Mosser et al. (2010). Similar age uncertainties are found here, despite using spectroscopic information – as we have now adopted not only individual uncertainties but also a more conservative uncertainty estimate for the seismic parameters (details can be found in Anders et al., in prep.).

The CoRoT-APOGEE sample (CoRoGEE) studied here is briefly described in Sect. 2, while a more detailed description can be found in Anders et al. (in prep.; hereafter A15). The latter paper describes the analysis performed to extract the main stellar properties for this sample, such as masses, radii, ages, distances, extinctions, and kinematic parameters. The authors also present some immediate results that can be obtained with the CoRoGEE sample, such as the variation of the disc metallicity gradient with time or age-chemistry relations outside the solar vicinity. In the present Letter, we focus on a group of stars which, despite being enhanced in [α/Fe], appear to be relatively young. Because these stars, at first sight, challenge the currently accepted paradigm, we carry out several tests to consolidate our assigned ages and abundances in our companion paper. In Sect. 3 we identify the young high-[α/Fe] stars and describe their main properties, and in Sect. 4 we discuss possible interpretations for their origin. Our main conclusions are summarised in Sect. 5.

2. Observations

The CoRoT data we employed are a subset of the larger sample analysed by Miglio et al. (2013a). Red-giant oscillation spectra have been analysed as in Mosser et al. (2010). The global seismic parameters $\Delta\nu$ and $\nu_{\rm max}$ were measured following the method described in Mosser & Appourchaux (2009). When possible, a more precise determination of the large spacing was derived from the correlation of the power spectrum with the universal red-giant oscillation pattern (Mosser et al. 2011). Outliers to the $\Delta\nu{-}\nu_{\rm max}$ relation, which would correspond to unrealistic stellar masses, were excluded.

These targets were observed by APOGEE, and the high-resolution infrared spectra were analysed with the APOGEE Stellar Parameter and Chemical Abundances Pipeline (ASPCAP; Mészáros et al. 2013; García Pérez et al., in prep.). Here, we adopted internally calibrated DR12 abundances (Holtzman et al. 2015; see more details in A15).

We used the Bayesian code PARAM (da Silva et al. 2006) to estimate stellar parameters. Masses, ages, distances, and extinctions were obtained with an updated version of the code (Rodrigues et al. 2014), which uses the combined photometric, seismic, and spectroscopic information to compute the probability density functions of these stellar properties. The final sample adopted here contains 622 red giant stars from the CoRoT LRa01 ($(l, b) = (212, -2)$) and LRc01 ($(l, b) = (37, -7)$) fields, for which a) high-quality spectroscopic criteria are fulfilled (APOGEE spectra with $S/N > 90$, $4000\,{\rm K} < T_{\rm eff} < 5300$ K, $1 < \log g < 3.5$); b) the PARAM code converged; and c) the seismic and calibrated spectroscopic $\log g$ are consistent within 0.5 dex. For this sample, median statistical uncertainties of about 0.02 dex in $\log g$, 4% in radius, 10% in mass, 25% in age, and 2.5% in distance were obtained (more details can be found in A15). As a caveat, stellar ages might still be affected by systematic uncertainties related to different stellar models and helium content, among other sources of errors (Lebreton et al. 2014; Lebreton & Goupil 2014; Martig et al. 2015; Miglio et al., in prep.).

Our dataset is complemented with similar information coming from two other high-resolution samples for which isochrone ages were available, the F & G solar-vicinity stars of Bensby et al. (2014), and the *Gaia*-ESO first internal data release of UVES spectra analysed in Bergemann et al. (2014). The total number of stars in each each sample is reported in Table 1.

Table 1. Abundance of young α-enhanced stars (yαr) in recent high-resolution spectroscopic surveys.

Sample	$R_{\rm Gal}$[a] [kpc]	N[b]	$1\sigma/2\sigma$ yαr
Fuhrmann[c], $d < 25$ pc	8	424	0/0
Bensby et al.[d]	8	714	8 (1.1%)/1 (0.1%)
GES[e], $\lvert Z_{\rm Gal}\rvert < 0.3$ kpc	6–9	55	0/0
GES[e], $\lvert Z_{\rm Gal}\rvert > 0.3$ kpc	6–9	91	3 (3.3%)/1 (1.1%)
LRa01[f]	9–14	288	3 (1.0%)/2 (0.7%)
LRc01[f], $\lvert Z_{\rm Gal}\rvert < 0.3$ kpc	6–7.5	151	4 (2.6%)/2 (1.3%)
LRc01[f], $\lvert Z_{\rm Gal}\rvert > 0.3$ kpc	4–6.5	183	21 (11.5%)/13 (7.1%)
APOKASC[g]	7–8	1639	14 (0.8%)

Notes. [a] Galactocentric range covered by different samples; [b] N = total number of stars in the sample; [c] The volume-complete sample of Fuhrmann (2011); [d] HIPPARCOS volume (Bensby et al. 2014); [e] *i*DR1 (Bergemann et al. 2014); [f] CoRoGEE, this work – see Appendix for detailed information on each star; [g] Martig et al. (2015). Outliers were defined in a different manner than in the present work.

3. Discovery of young [α/Fe]-rich stars in the Galactic disc

Figure 1 presents the age–[α/Fe] abundance relation for two local high-resolution spectroscopy samples: GES-UVES (Bergemann et al. 2014) and Bensby et al. (2014). The lower row shows the same relation for our CoRoGEE sample split into 1) outer-field (LRa01) stars; 2) inner-field (LRc01) stars with $Z_{\rm Gal} < 0.3$ kpc; and 3) inner-field stars with $Z_{\rm Gal} > 0.3$ kpc. The latter is necessary because for the inner field, stars of different heights below the mid-plane span different Galactocentric distance ranges. This behaviour is a consequence of the way the LRc01 CoRoT field was positioned (see Fig. 2; for more information on the population content of the LRc01 and LRa01 fields, see Miglio et al. 2013a).

We also show in Fig. 1 (upper-left panel) the predictions for the [Mg/Fe] vs. age chemical evolution of Chiappini (2009) for different Galactocentric annuli of the thick and thin discs. These models assume that the thick disc was formed on much shorter timescales and with a higher star formation efficiency than the thin disc. The shaded area corresponds to a parameter space not covered by a standard chemical evolution model of the thick and thin discs. Figure 1 demonstrates that while most of the data can be explained by standard chemical evolution models plus observational uncertainties (most probably accompanied by significant radial mixing, as discussed in Chiappini 2009; and Minchev et al. 2013, 2014), several stars are found to possess rather high [α/Fe] ratios, despite their young ages, and hence cannot be accounted for by the models. These stars are depicted as stars (1σ-outliers) and pentagons (2σ-outliers) in all figures. The young [α/Fe]-rich stars are more numerous in the inner field (see Fig. 2 and Table 1).

Table 1 shows the occurrance rates of young [α/Fe]-rich stars in the different analysed samples. Interestingly, there is a sudden rise in the fraction of young [α/Fe]-rich stars when smaller Galactocentric distances are sampled (which is the case of the CoRoT LRc01 field for $Z_{\rm Gal} > 0.3$ kpc), and the absence of these stars in the Fuhrmann (2011) sample, as well as other less volumed-confined samples such as Ramírez et al. (2007) – which might be due to a statistical effect.

The young [α/Fe]-rich stars cover a wide range of stellar parameters ($4200\,{\rm K} < T_{\rm eff} < 5100\,{\rm K}$, $1.7 < \log g < 2.7$; see also Fig. 10 of Martig et al. 2015). The abundance pattern of these stars compared to the entire CoRoGEE sample is displayed in

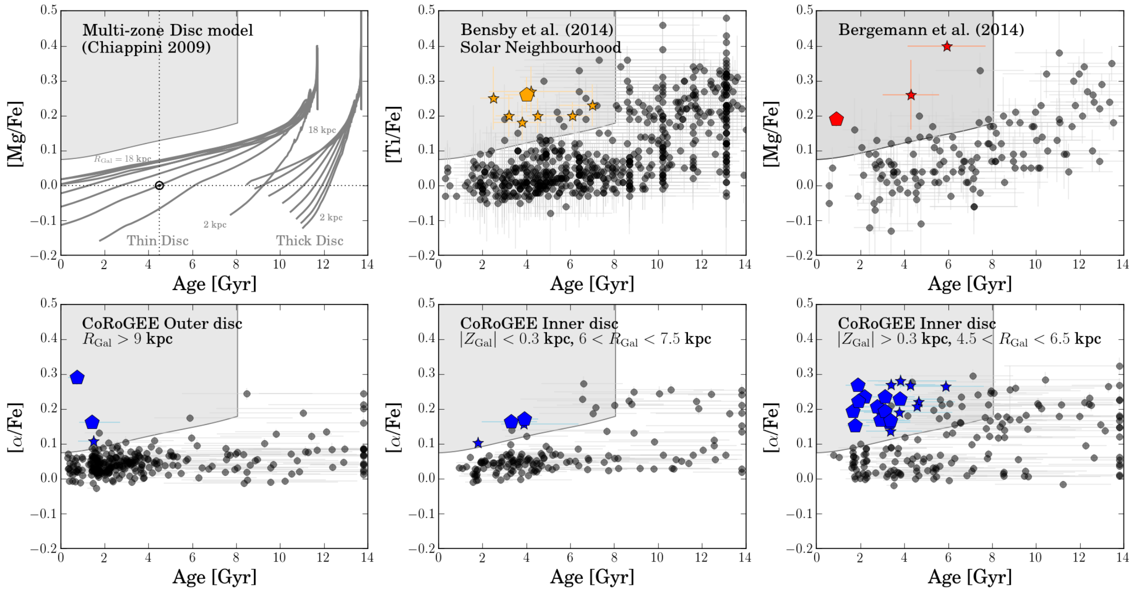

Fig. 1. Age–[α/Fe] relation in different regions of the Galactic disc. *Upper left panel*: the grey curves indicate the predictions of the multi-zone Galactic chemical-evolution model of Chiappini (2009) for the thin and thick discs, where different tracks were calculated for different Galactocentric annuli situated between 2 and 18 kpc from the Galactic Centre. The solar position is indicated in the diagram for the 6 kpc curve, the distance of the most probable birth position of the Sun (Minchev et al. 2013). Within these models, it is not possible to explain stars that fall into the grey-shaded region of the diagram: young, [α/Fe]-enhanced stars. The grey shadings provide a heuristic estimate of the typical $N\sigma$ ($N = 1, 2, 3$) uncertainties in [Mg/Fe] and age. *Upper middle and right panels*: the solar cylinder data from Bensby et al. (2014, *middle panel)* and the *Gaia*-ESO survey (Bergemann et al. 2014; *right panel*) show a clear correlation between isochrone-derived age estimates and relative [α/Fe] abundances. Stars whose age and abundance estimates are 1σ-incompatible with any of the chemical evolution curves are represented by stars; 2σ-outliers are represented by pentagons. *Lower panels*: the same diagram for the CoRoT-APOGEE sample. *Left*: the LRa01 outer-disc field. *Middle*: the LRc01 inner-disc field, close to the Galactic plane ($|Z_{\rm Gal}| < 0.3$ kpc, $R_{\rm Gal} > 6.0$ kpc). *Right*: the LRc01 field, below the Galactic plane ($Z_{\rm Gal} < -0.3$ kpc, $R_{\rm Gal} < 6.5$ kpc). In this region, the fraction of young α-enhanced stars is much larger than in all other regions. Considering *normal stars* alone, the age-[α/Fe] relation is much flatter than locally because the CoRoT stars span a wide range in Galactocentric distances.

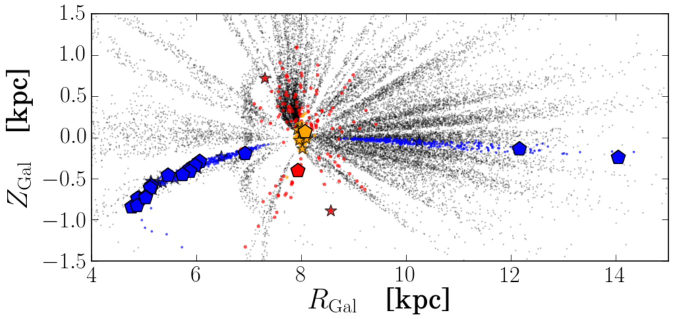

Fig. 2. Location of the APOGEE high-quality sample of Anders et al. (2014) in a $Z_{\rm Gal}$ vs. $R_{\rm Gal}$ plane (grey points). Also shown are the locations of the CoRoGEE stars (blue), the subgiant stars from Bergemann et al. (2014, red), and the Bensby et al. (2014) solar-vicinity dwarf stars (orange). As in Fig. 1, the discovered young [α/Fe]-rich stars are represented by the pentagons and stars.

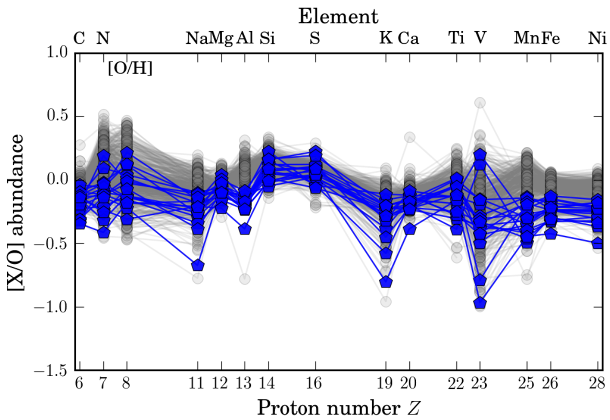

Fig. 3. Chemical-abundance patterns relative to oxygen for the CoRoGEE stars marked as chemically peculiar in Fig. 1 (blue hexagons, 2σ-outliers in the age–[α/Fe] diagram). The chemical abundance pattern of the rest of the CoRoGEE sample is presented in grey for comparison.

Fig. 3. These stars are compatible with being formed from a gas that has not been processed by many stellar generations, as indicated by the systematically lower abundance of iron-peak elements (lower contribution of type Ia supernovae to the chemical enrichment), as well as by the lower [N/O] and [C/O] abundance ratios (further indicating a mild contribution from intermediate-mass stars) with respect to the bulk of the CoRoGEE sample. However, when we restrict the comparison to stars with [O/H] < -0.2, no significant differences are detected any more.

We also investigated the kinematic properties of the young [α/Fe]-rich stars. Despite their [α/Fe] enhancements, many of them exhibit thin-disc like kinematics (although biased to hotter orbits because the inner CoRoT field samples Galactocentric distances below ~5 kpc only at larger distances from the mid-plane, $Z_{\rm Gal} > 0.3$ kpc). As a result of sample selection effects, stars with small Galactocentric distances are only reachable at large distances from the mid-plane and should not be mistaken for genuine thick-disc stars.

Focusing on the youngest stars (ages younger than 4 Gyr), where most of the 2σ outliers are found (see Fig. 1), we checked the locus of the young [α/Fe]-rich stars in the [Fe/H] vs. Galactocentric distance diagram (Fig. 4, left panel) and in the [Fe/H] vs. guiding radius diagram (Fig. 4, right panel). Similar to Minchev et al. (2014), we estimated the guiding-centre radius of

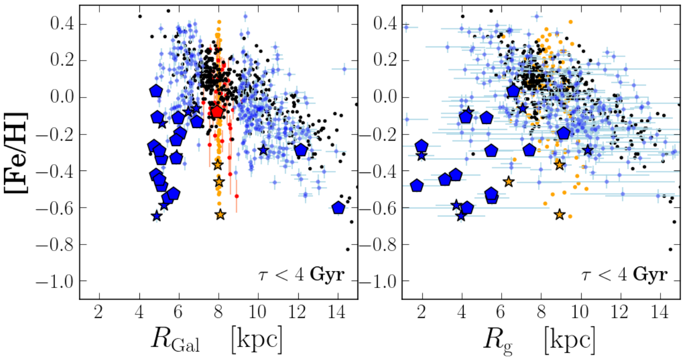

Fig. 4. Radial [Fe/H] distribution (*left*: as a function of Galactocentric distance $R_{\rm Gal}$, *right*: w.r.t. the guiding radius $R_{\rm g}$) over the extent of the Galactic disc (4−14 kpc range). As in Fig. 2, the CoRoGEE sample is shown in blue, the Bergemann et al. (2014) stars in red, and the Bensby et al. (2014) sample in orange. Again, hexagons and stars represent the young [α/Fe]-enhanced stars defined in Fig. 1. The locations of Galactic cepheids (black; data from Genovali et al. 2014) are also indicated.

a stellar orbit using the approximation $R_{\rm g} = \frac{L_z}{v_{\rm c}} = \frac{v_\phi \cdot R_{\rm Gal}}{v_{\rm c}}$, with L_z being the angular momentum, v_ϕ the ϕ-component of the space velocity in a Galactocentric cylindrical coordinate frame, and $v_{\rm c}$ the circular velocity at the star position – which for simplicity we assumed to be constant and equal to 220 km s^{-1} (see A15 for more details).

It is clear that most of the anomalous stars tend to be metal poor and to have small guiding radii ($R_{\rm g} \lesssim 6$ kpc – dashed line in Fig. 4). This is also the case of the young [α/Fe]-rich stars in the other two more local samples. In particular, a large number of these anomalous objects appear near the corotation region (with the caveat that there are large uncertainties in the estimate of the guiding radii). It is expected that as the age increases, more of these stars can also be found farther away from the corotation radius because radial migration would have had enough time to displace them from their birth position (Minchev et al. 2014). A larger age-baseline is discussed in A15, where we focus on the time evolution of abundance gradients.

4. What is their origin?

One possible interpretation is that the young [α/Fe]-rich stars might be evolved blue stragglers, that is, binary mergers. These have a higher mass and thus look like a young population. However, these stars should be present in all directions, at all metallicities, but in smaller numbers (see discussion in Martig et al. 2015).

The young α-rich stars appear to have been born from a relatively pristine gas, with metallicities above [Fe/H] ~ -0.7 (see Fig. 4, and Table A.1). One possibility is that these are objects formed from a recent gas accretion event. One caveat here is that outliers are also present in older age bins, suggesting that the processes responsible for creating these stars have been continuously working during the Milky Way evolution. A more plausible interpretation is to assume that the region near the bar corotation is the site for the formation of the young [α/Fe]-rich stars. In this region, gas can be kept inert for longer times than in other regions that are more often shocked by the passage of the spiral arms (Bissantz et al. 2003; Combes 2014). Additional dilution is expected from gas restored from the death of old low-mass stars in this inner-disc region (Minchev et al. 2013).

If this interpretation holds and the process is still taking place in a region near the end of the Galactic bar, we also expect to find young metal-poor, [α/Fe]-enhanced stars in that same region of the Galactic plane. Interestingly, there are some intriguing young objects in the MW that might be related to the same phenomenon: a) the puzzling low-metallicity supergiants located near the end of the Galactic bar (Davies et al. 2009a,b, see discussion in Genovali et al. 2014 and Origlia et al. 2013); b) the young [α/Fe]-enchanced stars reported by Cunha et al. (2007) near the Galactic Centre, and; c) the unusual Cepheid BC Aql which, despite being young (Whitelock, priv. comm.) and located at $R_{\rm Gal} \sim 5$ kpc, is also [α/Fe]-enhanced and metal-poor (Luck & Lambert 2011). Other Cepheids, recently discovered far from the Galactic plane on the opposite side of the Galaxy (Feast et al. 2014), also appear to be young (i.e., their period-age relations are compatible with ages $\lesssim$130 Myr).

Within our framework, we expect similar stars to have been forming in that same region (i.e., near the bar corotation) for the past 4–5 Gyr. As extensively discussed by Minchev et al. (2013, 2014), stars born at the corotation radius have a high probability of being expelled to an outer region via radial migration. This result suggests that the mechanism proposed here could have a strong effect on the thin disc by contaminating the entire disc with this metal-poor and [α/Fe]-rich population and that it might be related to the observed [Fe/H] ~ -0.7 *floor* in the abundance gradients. One possible observable signature of this process might be the intermediate-age α-enhanced open clusters found by Yong et al. (2012, and references therein).

5. Conclusions

In this Letter we reported the discovery of young [α/Fe]-enhanced stars in a sample of CoRoT stars observed by APOGEE (CoRoGEE). These stars have a lower iron-peak element content than the rest of the CoRoGEE sample and are more abundant towards the inner Galactic disc regions. Almost all of the young [α/Fe]-rich stars we discovered have guiding radii $R_{\rm g} \leq 6$ kpc. Therefore, we tentatively suggest that the origin of these stars is related to the complex chemical evolution that takes place near the corotation region of the Galactic bar.

Unfortunately, some ambiguity remains because the inner Galactic regions accessible to CoRoT are above $|Z_{\rm Gal}| = 0.3$ kpc. This situation is expected to improve by combining future APOGEE-2 data with *Kepler* seismology from the K2 Campaign (Howell et al. 2014), a goal for SDSS-IV. Further into the future, more information will be obtained from *Gaia* and the PLATO-2 mission (Rauer et al. 2014), both complemented by spectroscopy for example with the 4MOST facility (de Jong et al. 2014).

In a companion paper (Martig et al. 2015), we report the discovery of young-[α/Fe]-rich stars in the *Kepler* field (although in smaller numbers). Finally, in an ongoing *Gaia*-ESO follow-up of the CoRoT inner-field stars, more of these stars are found (Valentini et al., in prep.), providing better statistics and complementing the results shown in this Letter.

Acknowledgements. The CoRoT space mission, launched on December 27 2006, was developed and operated by CNES, with the contribution of Austria, Belgium, Brazil, ESA (RSSD and Science Program), Germany and Spain. C.C. thanks A. Baglin, J. Storm and G. Cescutti for helpful discussions. T.S.R. acknowledges support from CNPq-Brazil. L.G. acknowledges support from PRIN INAF 2014. T.M. acknowledges financial support from Belspo for contract PRODEX *Gaia*-DPAC. S.M. acknowledges the support of the NASA grant NNX12AE17G. T.C.B. acknowledges partial support from grants PHY 08-22648; Physics Frontier Center/JINA, and PHY 14-30152; Physics Frontier Center/JINA Center for the Evolution of the Elements (JINA-CEE), awarded by the US National Science Foundation. The research leading to the presented results has received funding from the European Research Council under the European Community's Seventh Framework Programme (FP7/2007-2013) / ERC grant agreement No. 338251 (StellarAges). Funding for the SDSS-III Brazilian Participation Group has been provided by the Ministério de Ciência e Tecnologia (MCT), Fundação Carlos

Chagas Filho de Amparo à Pesquisa do Estado do Rio de Janeiro (FAPERJ), Conselho Nacional de Desenvolvimento Científico e Tecnológico (CNPq), and Financiadora de Estudos e Projetos (FINEP). Funding for SDSS-III has been provided by the Alfred P. Sloan Foundation, the Participating Institutions, the National Science Foundation, and the US Department of Energy Office of Science. The SDSS-III web site is http://www.sdss3.org/. SDSS-III is managed by the Astrophysical Research Consortium for the Participating Institutions of the SDSS-III Collaboration including the University of Arizona, the Brazilian Participation Group, Brookhaven National Laboratory, Carnegie Mellon University, University of Florida, the French Participation Group, the German Participation Group, Harvard University, the Instituto de Astrofisica de Canarias, the Michigan State/Notre Dame/JINA Participation Group, Johns Hopkins University, Lawrence Berkeley National Laboratory, Max Planck Institute for Astrophysics, Max Planck Institute for Extraterrestrial Physics, New Mexico State University, New York University, Ohio State University, Pennsylvania State University, University of Portsmouth, Princeton University, the Spanish Participation Group, University of Tokyo, University of Utah, Vanderbilt University, University of Virginia, University of Washington, and Yale University.

References

Alam, S., Albareti, F. D., Allende Prieto, C., et al. 2015, ApJS, submitted [arXiv:1501.00963]
Anders, F., Chiappini, C., Santiago, B. X., et al. 2014, A&A, 564, A115
Baglin, A., Auvergne, M., Barge, P., et al. 2006, in ESA SP 1306, eds. M. Fridlund, A. Baglin, J. Lochard, & L. Conroy, 33
Bensby, T., Feltzing, S., & Oey, M. S. 2014, A&A, 562, A71
Bergemann, M., Ruchti, G. R., Serenelli, A., et al. 2014, A&A, 565, A89
Bissantz, N., Englmaier, P., & Gerhard, O. 2003, MNRAS, 340, 949
Chiappini, C. 2009, in IAU Symp. 254, eds. J. Andersen, B. Nordström, & J. Bland-Hawthorn, 191
Chiappini, C., Matteucci, F., & Gratton, R. 1997, ApJ, 477, 765
Combes, F. 2014, in Structure and Dynamics of Disk Galaxies, eds. M. S. Seigar, & P. Treuthardt, ASP Conf. Ser., 480, 211
Cunha, K., Sellgren, K., Smith, V. V., et al. 2007, ApJ, 669, 1011
da Silva, L., Girardi, L., Pasquini, L., et al. 2006, A&A, 458, 609
Davies, B., Origlia, L., Kudritzki, R.-P., et al. 2009a, ApJ, 694, 46
Davies, B., Origlia, L., Kudritzki, R.-P., et al. 2009b, ApJ, 696, 2014
de Jong, R. S., Barden, S., Bellido-Tirado, O., et al. 2014, in SPIE Conf. Ser., 9147
Eisenstein, D. J., Weinberg, D. H., Agol, E., et al. 2011, AJ, 142, 72
Feast, M. W., Menzies, J. W., Matsunaga, N., & Whitelock, P. A. 2014, Nature, 509, 342
Fuhrmann, K. 2011, MNRAS, 414, 2893
Genovali, K., Lemasle, B., Bono, G., et al. 2014, A&A, 566, A37
Gilliland, R. L., Brown, T. M., Christensen-Dalsgaard, J., et al. 2010, PASP, 122, 131
Gunn, J. E., Siegmund, W. A., Mannery, E. J., et al. 2006, AJ, 131, 2332
Haywood, M., Di Matteo, P., Lehnert, M. D., Katz, D., & Gómez, A. 2013, A&A, 560, A109
Holtzman, J. A., Shetrone, M., Johnson, J. A., et al. 2015, AJ, submitted [arXiv:1501.04110]
Howell, S. B., Sobeck, C., Haas, M., et al. 2014, PASP, 126, 398
Lebreton, Y., & Goupil, M.-J. 2014, A&A, 569, A21
Lebreton, Y., Goupil, M. J., & Montalbán, J. 2014, in EAS Pub. Ser., 65, 99
Luck, R. E., & Lambert, D. L. 2011, AJ, 142, 136
Martig, M., Rix, H.-W., Silva Aguirre, V., et al. 2015, MNRAS, submitted [arXiv:1412.3453]
Matteucci, F. 2001, The chemical evolution of the Galaxy, Astrophys. Space Sci. Libr., 253
Mészáros, S., Holtzman, J., García Pérez, A. E., et al. 2013, AJ, 146, 133
Miglio, A., Chiappini, C., Morel, T., et al. 2013a, MNRAS, 429, 423
Miglio, A., Chiappini, C., Morel, T., et al. 2013b, in EPJ Web Conf., 43, 3004
Minchev, I., Chiappini, C., & Martig, M. 2013, A&A, 558, A9
Minchev, I., Chiappini, C., & Martig, M. 2014, A&A, 572, A92
Mosser, B., & Appourchaux, T. 2009, A&A, 508, 877
Mosser, B., Belkacem, K., Goupil, M.-J., et al. 2010, A&A, 517, A22
Mosser, B., Barban, C., Montalbán, J., et al. 2011, A&A, 532, A86
Origlia, L., Oliva, E., Maiolino, R., et al. 2013, A&A, 560, A46
Pagel, B. E. J. 2009, Nucleosynthesis and Chemical Evolution of Galaxies (Cambridge, UK: Cambridge University Press)
Ramírez, I., Allende Prieto, C., & Lambert, D. L. 2007, A&A, 465, 271
Rauer, H., Catala, C., Aerts, C., et al. 2014, Exp. Astron., 38, 249
Rodrigues, T. S., Girardi, L., Miglio, A., et al. 2014, MNRAS, 445, 2758
Yong, D., Carney, B. W., & Friel, E. D. 2012, AJ, 144, 95

[1] Leibniz-Institut für Astrophysik Potsdam (AIP), An der Sternwarte 16, 14482 Potsdam, Germany
e-mail: Cristina.Chiappini@aip.de
[2] Laboratório Interinstitucional de e-Astronomia, – LIneA, Rua Gal. José Cristino 77, 20921-400 Rio de Janeiro, Brazil
[3] Osservatorio Astronomico di Padova – INAF, Vicolo dell'Osservatorio 5, 35122 Padova, Italy
[4] Dipartimento di Fisica e Astronomia, Università di Padova, Vicolo dell'Osservatorio 3, 35122 Padova, Italy
[5] School of Physics and Astronomy, University of Birmingham, Edgbaston, Birmingham, B15 2TT, UK
[6] LESIA, Université Pierre et Marie Curie, Université Denis Diderot, Obs. de Paris, 92195 Meudon Cedex, France
[7] Institut d'Astrophysique et de Geophysique, Allée du 6 août, 17 – Bât. B5c, 4000 Liège 1 (Sart-Tilman), Belgium
[8] Instituto de Física, Universidade Federal do Rio Grande do Sul, Caixa Postal 15051, 91501-970 Porto Alegre, Brazil
[9] Observatoire de la Côte d'Azur, Laboratoire Lagrange, CNRS UMR 7923, BP 4229, 06304 Nice Cedex, France
[10] Max-Planck-Institut für Astronomie, Königstuhl 17, 69117 Heidelberg, Germany
[11] Observatório Nacional, Rua Gal. José Cristino 77, 20921-400 Rio de Janeiro, Brazil
[12] Instituto de Astrofísica de Canarias, 38205 La Laguna, Tenerife, Spain
[13] Universidad de La Laguna, Departamento de Astrofísica, 38206 La Laguna, Tenerife, Spain
[14] Max-Planck-Institut für Sonnensystemforschung, Justus-von-Liebig-Weg 3, 37077 Göttingen, Germany
[15] Stellar Astrophysics Centre, Department of Physics and Astronomy, Aarhus University, Ny Munkegade 120, 8000 Aarhus C, Denmark
[16] Institut für Astronomie, Universität Wien, Türkenschanzstr. 17, 1180 Wien, Austria
[17] Laboratoire AIM, CEA/DSM – CNRS – Univ. Paris Diderot – IRFU/SAp, Centre de Saclay, 91191 Gif-sur-Yvette Cedex, France
[18] Space Science Institute, 4750 Walnut Street Suite 205, Boulder CO 80301, USA
[19] Institut d´Astrophysique Spatiale, UMR8617, CNRS, Université Paris XI, Bâtiment 121, 91405 Orsay Cedex, France
[20] Dept. of Physics and JINA-CEE: Joint Institute for Nuclear Astrophysics – Center for the Evolution of the Elements, Univ. of Notre Dame, Notre Dame, IN 46530, USA
[21] 57 Department of Astronomy, Case Western Reserve University, Cleveland, OH 44106, USA
[22] New Mexico State University, Las Cruces, NM 88003, USA
[23] Department of Astronomy, University of Virginia, PO Box 400325, Charlottesville VA 22904-4325, USA
[24] ELTE Gothard Astrophysical Observatory, 9704 Szombathely, Szent Imre herceg st. 112, Hungary
[25] Department of Astronomy, Indiana University, Bloomington, IN 47405, USA
[26] Dept. of Astronomy, University of Michigan, Ann Arbor, MI 48104, USA
[27] Apache Point Observatory PO Box 59, Sunspot, NM 88349, USA
[28] Astrophysics Research Institute, Liverpool John Moores University, IC2, Liverpool Science Park 146 Brownlow Hill Liverpool L3 5RF, UK
[29] McDonald Observatory, University of Texas at Austin, HC75 Box 1337-MCD, Fort Davis, TX 79734, USA
[30] Department of Astronomy and Astrophysics, The Pennsylvania State University, University Park, PA 16802, USA
[31] Institute for Gravitation and the Cosmos, The Pennsylvania State University, University Park, PA 16802, USA
[32] Vanderbilt University, Dept. of Physics & Astronomy, VU Station B 1807, Nashville, TN 37235, USA

Pages 6 to 7 are available in the electronic edition of the journal at http://www.aanda.org

Appendix A: Best-candidate young α-enhanced stars in the CoRoGEE sample

Table A.1 summarises our measured quantities for the best-candidate young α-enhanced stars (17 2σ-outliers; blue large pentagons in Fig. 1, and 11 1σ-outliers; blue stars in Fig. 1). We first report our input values: the adopted seismic parameters $\Delta\nu$ and $\nu_{\rm max}$ (as computed by automatic as well as supervised analyses of the CoRoT light curves), ASPCAP spectroscopic parameters $T_{\rm eff}$, [Fe/H], [α/Fe], and the number of APOGEE observations, $N_{\rm APO}$. We note that all stars in question have been observed at very high signal-to-noise ratios ($S/N > 140$ per resolution element). The radial-velocity scatter between subsequent observations is always smaller than 0.6 km s^{-1}; meaning that their values are consistent with all stars being single stars or widely separated binaries.

We also present the estimated stellar masses $M_{\rm scale}$, as determined from seismic scaling relations and the 1σ upper-limits for the ages (as determined by PARAM). A comparison of the masses estimated by PARAM and those inferred directly from the scaling relations is reported in A15 for the full CoRoGEE sample. Also listed are the current Galactocentric positions $R_{\rm Gal}$ and $Z_{\rm Gal}$ and the guiding radius $R_{\rm g}$ of each star.

We also show a note on the quality of the light curves (Q) and a flag based on the supervised analysis. Because the automated and supervised analyses sometimes yield different results, we recomputed masses and ages using the individually obtained $\Delta\nu$ and $\nu_{\rm max}$ values and updated uncertainties where necessary. As expected, the numbers of the young α-enhanced stars are slightly different. In Table A.1, we only report the robust 2σ- and 1σ-outliers.

The individual supervised analysis shows that:

1. After the individual analysis, still 28 stars out of 39 candidates fulfilled our outlier criterion;
2. Four stars that seemed to be 2σ-outliers were shifted to older ages: CoRoT 101093867, 101071033, 102645343, and 10264381. Similarly, seven candidate 1σ-outliers fall out of the sample: CoRoT 101057962, 101041814, 102626343, 100886873, 101208801, 101212022, and 101227666.
3. One star (CoRoT 101071033) had to be excluded from the parent sample due to the very poor quality of its light curve;
4. CoRoT 101093867 is a complex case, where both $\Delta\nu$ values appear as possible solutions; for six other stars, another solution is possible, because the light curve S/N is not high enough to undoubtedly resolve the radial/dipole mode possible mismatch (such cases cannot be seen in the general blind automated analysis);
5. For CoRoT 100958571, the solution obtained through supervised fitting, close to the one found by the automated pipeline, should be preferred. Also, for most of the remaining stars, slight improvements in the determination of the seismic parameters are possible.

Table A.1. Best-candidate young α-enhanced stars: seismic and spectroscopic adopted parameters and uncertainties, stellar masses and ages, current Galactocentric positions $R_{\rm Gal}$ and $Z_{\rm Gal}$, and guiding-centre radii $R_{\rm g}$.

CoRoT ID	APOGEE ID	$\Delta\nu$ [μHz]	$\nu_{\rm max}$ [μHz]	Q^a	$\Delta\nu_i{}^b$ [μHz]	$\nu_{{\rm max}_i}{}^b$ [μHz]	Flag^c	$N_{\rm APO}$	$T_{\rm eff}{}^d$ [K]	[Fe/H]	[α/Fe]	$M_{\rm scale}$ [$M_\odot$]	$\tau_{\rm 68U}{}^e$ [Gyr]	$\tau^{\rm i}_{\rm 68U}{}^f$ [Gyr]	$R_{\rm Gal}{}^g$ [kpc]	$Z_{\rm Gal}{}^h$ [kpc]	$R_{\rm g}$ [kpc]
							2σ-outliers										
100580176	2M19232036+0116385	1.2 ± 0.01	8.11 ± 0.22	OK	1.27	8.0	1	1	4200	−0.2 ± 0.03	0.16 ± 0.01	1.49 ± 0.22	2.5	4.5	6.06	−0.29	9.1 ± 0.5
100692726	2M19240121+0115468	2.71 ± 0.03	22.41 ± 0.58	OK	2.7	22.3	0	7	4390	−0.11 ± 0.03	0.16 ± 0.01	1.48 ± 0.14	4.3	4.3	4.91	−0.75	4.2 ± 1.2
100958571	2M19253009+0100237	1.94 ± 0.04	14.72 ± 0.65	OK	1.97	14.7	2	3	4410	−0.55 ± 0.04	0.20 ± 0.02	1.51 ± 0.24	3.4	4.7	5.46	−0.46	5.5 ± 0.9
101045095	2M19260245+0003446	2.78 ± 0.04	22.17 ± 0.64	poor	2.8	22.6	0	3	4400	−0.23 ± 0.03	0.23 ± 0.01	1.34 ± 0.14	6.0	5.7	5.87	−0.38	
101072104	2M19261545+0011507	3.01 ± 0.04	23.90 ± 0.71	OK	3.01	24.8	0	7	4580	−0.42 ± 0.04	0.24 ± 0.02	1.41 ± 0.14	5.8	3.6	4.87	−0.74	3.7 ± 1.2
101100354	2M19262657+0144163	4.56 ± 0.04	41.60 ± 0.93	poor	4.34	43.6	2	7	4520	−0.12 ± 0.03	0.21 ± 0.01	1.74 ± 0.14	7.6	3.0	5.97	−0.34	5.3 ± 0.7
101113416	2M19263149+0159448	1.11 ± 0.01	6.79 ± 0.20	OK	1.14	6.74	1	3	4360	−0.48 ± 0.04	0.24 ± 0.02	1.36 ± 0.15	3.6	4.5	5.14	−0.58	1.7 ± 1.2
101114706	2M19263197-0035004	0.97 ± 0.02	6.14 ± 0.31	OK	0.98	6.14	0	3	4170	−0.27 ± 0.03	0.19 ± 0.01	1.65 ± 0.29	3.5	3.8	4.76	−0.84	2.0 ± 1.0
101121769	2M19263465+0004069	1.34 ± 0.03	8.88 ± 0.35	OK	1.34	8.88	0	3	4340	−0.34 ± 0.03	0.17 ± 0.02	1.52 ± 0.23	4.0	4.0	5.12	−0.61	
101138968	2M19264111+0214048	2.46 ± 0.04	20.74 ± 0.73	OK	2.46	20.7	0	7	4500	−0.45 ± 0.04	0.27 ± 0.02	1.79 ± 0.22	2.1	2.3	5.03	−0.72	3.2 ± 1.1
101342375	2M19280053+0016331	2.06 ± 0.04	16.69 ± 0.74	OK	2.00	16.7	0	7	4340	0.03 ± 0.03	0.15 ± 0.01	2.03 ± 0.32	2.6	2.4	4.86	−0.83	6.6 ± 1.2
101386073	2M19282189+0010322	5.21 ± 0.07	48.40 ± 1.41	OK	5.23	51.2	0	7	4610	−0.33 ± 0.04	0.19 ± 0.02	1.37 ± 0.14	6.9	3.9	5.87	−0.41	
101415638	2M19283410+0006205	5.21 ± 0.11	47.68 ± 2.28	poor	4.80	47.7	1	7	4960	−0.53 ± 0.04	0.22 ± 0.02	1.48 ± 0.32	2.7	2.1	5.74	−0.45	5.5 ± 0.7
101594554	2M19294723+0007020	2.70 ± 0.03	21.52 ± 0.51	OK	2.72	21.73	0	7	4430	−0.29 ± 0.04	0.17 ± 0.01	1.35 ± 0.11	4.4	4.3	5.03	−0.73	5.5 ± 1.1
101748322	2M19305707-0008228	5.55 ± 0.03	53.17 ± 0.84	OK	5.40	52.4	2	3	4710	−0.14 ± 0.03	0.17 ± 0.01	1.34 ± 0.08	5.5	4.5	6.93	−0.19	
102673776	2M06430619-0103534	2.23 ± 0.05	16.83 ± 0.77	OK	2.23	16.8	0	4	5070	−0.61 ± 0.04	0.29 ± 0.02	1.69 ± 0.28	0.8	0.8	14.05	−0.25	4.3 ± 4.2
102733615	2M06442450-0100460	3.33 ± 0.09	30.93 ± 1.85	poor	3.06	30.9	1	4	4760	−0.29 ± 0.04	0.16 ± 0.02	2.28 ± 0.56	3.2	2.7	12.16	−0.14	7.4 ± 2.5
							1σ-outliers										
100667041	2M19235081+0111425	2.5 ± 0.03	19.85 ± 0.46	OK	2.59	19.8	2	7	4400	−0.34 ± 0.04	0.22 ± 0.02	1.23 ± 0.11	4.1	6.3	5.13	−0.53	
100889852	2M19250803+0152285	5.47 ± 0.1	53.41 ± 2.25	poor	5.62	56.1	2	7	4620	−0.32 ± 0.04	0.27 ± 0.02	1.36 ± 0.19	6.0	5.4	5.92	−0.33	2.0 ± 0.7
101029567	2M19255543+0014035	2.33 ± 0.04	17.76 ± 0.81	OK	2.35	17.7	0	7	4490	−0.65 ± 0.04	0.28 ± 0.02	1.34 ± 0.21	5.8	6.4	4.9	−0.71	4.0 ± 1.2
101073282	2M19261630+0116446	5.63 ± 0.09	56.33 ± 2.01	OK	5.53	56.9	0	3	4900	−0.08 ± 0.03	0.10 ± 0.01	1.65 ± 0.21	1.8	1.9	6.48	−0.24	4.3 ± 0.5
101200652	2M19270430+0120124	2.23 ± 0.04	17.11 ± 0.70	poor	2.36	17.5	1	7	4500	−0.59 ± 0.04	0.19 ± 0.02	1.38 ± 0.23	3.8	6.2	5.27	−0.55	3.7 ± 1.0
101364068	2M19281113-0020004	2.83 ± 0.04	21.34 ± 0.68	OK	2.84	22.2	0	3	4650	−0.21 ± 0.04	0.21 ± 0.01	1.30 ± 0.15	8.0	5.9	6.03	−0.38	2.8 ± 0.5
101392012	2M19282435+0117076	1.47 ± 0.02	9.12 ± 0.25	OK	1.50	9.06	1	3	4390	−0.65 ± 0.04	0.26 ± 0.02	1.10 ± 0.10	6.2	7.6	5.35	−0.55	4.5 ± 1.0
101419125	2M19283555-0013131	6.40 ± 0.09	63.78 ± 2.14	poor	6.57	65.8	1	7	4810	−0.49 ± 0.04	0.27 ± 0.02	1.25 ± 0.15	5.9	5.8	5.58	−0.50	4.9 ± 0.8
101476920	2M19285918+0036543	2.20 ± 0.03	16.63 ± 0.54	OK	2.25	17.3	0	7	4410	−0.14 ± 0.03	0.14 ± 0.01	1.45 ± 0.16	5.1	4.8	5.17	−0.64	
101665008	2M19302198+0018463	6.02 ± 0.05	61.93 ± 1.35	OK	6.30	62.6	1	3	4600	−0.06 ± 0.03	0.16 ± 0.01	1.28 ± 0.15	4.3	6.4	6.88	−0.20	7.1 ± 0.3
102768182	2M06451106-0032468	2.94 ± 0.06	27.18 ± 1.29	poor	2.94	27.0	0	3	4840	−0.29 ± 0.04	0.11 ± 0.02	2.17 ± 0.37	1.7	1.7	10.25	−0.05	10.3 ± 0.5

Notes. [(a)] Quality of CoRoT light curve and the automated global fits; [(b)] Results of individual supervised fit to the light curves; [(c)] Flag on supervised fits (0 = automated and supervised fit are consistent within 1σ. 1 = there are two possible solutions for $\Delta\nu$ or $\nu_{\rm max}$, due to the ambiguity of radial and dipole oscillation modes. 2 = supervised fit yields improved results); [(d)] Overall uncertainties: $\sigma T_{\rm eff}$ = 91 K (Holtzman et al. 2015); [(e)] 1σ age upper limit, using the seismic results from the automatic pipeline; [(f)] 1σ age upper limit, using the seismic results from the supervised seismic analysis; [(g)] Typical uncertainties: ~0.1 kpc, for the most distant stars in LRa01 ~ 0.5 kpc; [(h)] Typical uncertainties: <0.1 kpc, for the most distant stars in LRc01 ~ 0.4 kpc.